

Plasma Nitriding of ISO 5832-1 Stainless Steel at 425 °C with Intermittent Nitrogen Flow

Andrey Matheus Vianna^a, Cristiano Brunetti^b , Marcio Mafra^a , Ricardo Fernando dos Reis^a ,

Rodrigo Luppini Villanova^a , Euclides Alexandre Bernardelli^{a*} 

^aUniversidade Tecnológica Federal do Paraná (UTFPR), Curitiba, PR, Brasil

^bInstituto Federal do Paraná (IFPR), Paranaguá, PR, Brasil

Received: June 07, 2020; Revised: September 01, 2020; Accepted: September 06, 2020

The aim of this work was to study the influence of varying nitrogen potential during plasma nitriding of stainless steel ISO 5832-1. The control of nitrogen potential was achieved by pulsing the nitrogen flow for different times (01/19, 02/18, and 05/15), where the numbers represent the time (in minutes) of nitrogen flow on/off, thus creating an intermittent flow of nitrogen during the treatment. For all tested conditions - continuous and pulsed flow of nitrogen - the treatment temperature was kept at 425°C during 2 and 8 hours. Specimens were characterized by means of X-ray diffraction, scanning electron microscopy, optical microscopy, energy-dispersive X-ray spectroscopy, and nanohardness. Results showed that the layer thickness increases with the increase of total treatment time, and decreased for shorter times of pulsed nitrogen flow. Smaller expansion of the austenite phase, as well as less precipitation of chromium nitrides, were also observed for shorter times of pulsed nitrogen flow. Hence, the use of intermittent nitrogen flow appears to be an efficient approach in order to control the nitrogen concentration within the layer, reducing its brittleness.

Keywords: *stainless steels, ISO 5832-1, plasma nitriding, nitrogen potential.*

1. Introduction

Stainless steels have a broad range of applications in the industry because of their high corrosion resistance. However, both mechanical strength and wear resistance of the majority of stainless steels are poor when compared to carbon steels¹⁻¹⁰. In order to overcome such limitations, several works regarding thermochemical treatments have been developed, specially plasma nitriding, which is largely used in academic and industrial fields^{5, 9-12}. When the plasma nitriding process is carried out at temperatures below 400°C, a metastable phase known as expanded austenite (γ_N)^{1-8, 10-19} or S-phase^{1-6, 10, 12, 15-19} is formed. This phase improves mechanical strength and wear and fatigue resistance, and even corrosion resistance in some cases^{1-8, 10-19}. However, when nitriding is carried out at such low temperatures, the formed layer is very thin, limiting its use in certain applications.

Plasma nitriding of stainless steels should be made at temperatures around 400°C in order to avoid or reduce significantly the formation of precipitates such as chromium nitride (CrN). Such precipitates depletes it surrounding regions in chromium, thus reducing drastically the corrosion resistance of the steel^{2, 3, 5-8, 19, 20}. Another related issue is the excessive hardness of the formed layer caused by the high level of compressive stresses resulting from austenite expansion, which can lead to the formation of cracks within the layer^{8, 12, 14}.

Aiming to decrease the brittleness of the nitrided layer, Sphair et al¹ conducted nitriding processes with intermittent

flow of nitrogen, and they showed that it was possible to control the nitrogen amount in the expanded austenite, and that the expansion of the austenite was smaller for shorter times of nitrogen flow. From these results, one can see the opportunity to control the precipitation of chromium nitride by using intermittent nitrogen flow as well, even at a temperature where this precipitation occurs. Controlling the precipitation arrives from the fact that the formation of chromium nitride is influenced both by temperature^{6, 9, 11} and nitrogen concentration^{8, 17}.

In the work made by Reis et al², nitriding of ISO 5832-1 stainless steel was carried out at 450°C, and the authors observed that the amount of chromium nitrides decreased with the use of intermittent nitrogen flow; however, it did not avoid their precipitation. In their paper, they suggest that the nitriding process could be made at lower temperatures to avoid such precipitation.

The use of gas pulses, as shown by Sphair²¹, has economic advantages when compares to the use of continuous gas flow, since it is possible to produce less brittle layers with lower probability of crack formation at the same time that it is possible to make the process at temperatures higher than 400°C, allowing to obtain higher thickness layers with minimum nitrides precipitation²². Regarding gas consumption, Sphair²¹ observed that the savings are not significant for a 2 hours process carried out according to the experimental conditions of the referred work.

Hence, the aim of the present work was to determine the influence of intermittent flow of nitrogen on the characteristics of ISO 5832-1 stainless steel nitrided at 425°C.

*e-mail: ebernardelli@utfpr.edu.br

2. Experimental Procedures

The material used in this work was obtained from a drawn bar with diameter of 12.7 mm of ISO 5832-1 stainless steel. The chemical composition of the material is shown in Table 1. Initially the bar was submitted to a solubilization heat treatment at 1100°C for 2 hours, and then specimens with 6 mm height were cut from the solubilized bar. After cutting, the surface of the specimens was ground with emery paper and ultrasonic cleaned with 98 GL alcohol for 5 minutes. Specimens were then polished with 1 μm alumina suspension and ultrasonic cleaned again after polishing.

Table 2 shows the parameters used in the nitriding processes. A plasma reactor and a DC power supply with PWM (Pulse Width Modulation) of the UTFPR Plasma Laboratory (LabPlasma) were used to conduct the nitriding processes. Before nitriding, an in situ cleaning process was carried out with an atmosphere composed of 33% H_2 and 66% Ar and total flow of 150 sccm for 20 minutes. The parameters that were varied in the nitriding processes were total cycle time and nitrogen pulse time, while remaining parameters were kept unchanged for all nitriding cycles. The pressure was manually adjusted in order to compensate the changes in gas flow and to keep it constant at 3 Torr. The identification scheme of the specimens is illustrated in Figure 1.

The choice of gas pulse times (gas flow on) was based on the mass flow controller (MFC) installed in the experimental device, which has a response time of 0.5 minutes between the valve start and its actual opening. Hence, the minimum possible time of gas flow on is 0.5 minutes, which was the initial chosen time for the condition P0119. The times of gas flow on for the other conditions were then tripled regarding previous conditions, that is, for the condition P0218 it was 1.5 minutes, and for condition P0515 it was 4.5 minutes. In her work, Sphair²¹ shows an optical emission spectroscopy graph where it is possible to see the time needed between

to cease the emission of nitrogen species and the MFC shut down, and the time needed to start nitrogen species emission after the MFC is turned on. In that work, the term “nitrogen potential” is related to the intensity of optical emission of nitrogen species; when the MFC is turned on, there is a high nitrogen potential, when the MFC is turned off, there is a low nitrogen potential.

The electrical potential difference was kept constant because it is a control parameter of the high voltage source. Since it is a PWM (Pulse Width Modulation) controlled source, it is possible to adjust both t_{on} and t_{off} (pulse time on and pulse time off, respectively). The T_{off} was kept constant at 200 μs for all treatments, while t_{on} varied from 60 μs when the nitrogen flow was on to 40 μs when the nitrogen flow was interrupted. Such control was necessary in order to keep the process temperature stable at 425°C.

After nitriding, specimens were characterized by X-ray diffraction (XRD) in a Shimadzu XRD-6100 diffractometer from Federal Institute of Paraná, Paranaguá Campus. The following parameters were employed: Cu α radiation ($\lambda = 1.5418\text{\AA}$), current of 2 mA, and voltage of 40 kV. Scan rate was 1°/min for a 2θ ranging from 30° to 100°. The software X'Pert Highscore Plus was used for phase identification. The following crystallographic cards were used to identify the phases present on the nitrided layer: card n° 06-0627 (Fe_4N); card n° 01-1216 (Fe_3N); card n° 11-0065 (CrN); and card n° 35-0803 (Cr_2N).

The nanohardness technique was used to evaluate the surface hardness of the nitrided specimens. Such measurements were carried out at Federal University of Paraná with the aid of a model ZHN Zwick Roell equipment. Tests were made according to the QCSM (Quasi Continuous Stiffness Measurement) method, where the load is applied in increasing small steps with a diamond indenter. A maximum load of 100 mN was used, and 25 measurements were made for each specimen.

Table 1. Chemical composition of ISO 5832-1 austenitic stainless steel (wt%) (Sphair²¹)

C	Mn	P	S	Si	Cr	Ni	Mo	Al	V	Cu	Fe
0.012	1.66	0.017	0.018	0.28	17.1	10.6	1.67	0.011	0.074	0.702	Bal.

Table 2. Summary of the process parameters.

Temperature (°C)	t_{on} (μs)	t_{off} (μs)	Voltage (V)	Gas flow (sccm)	Pressure (torr)	Treatment time (h)	Duration of N_2 pulse (on/off) (min)	Code
425 \pm 3	50 \pm 10	200	500	200 (25% N_2 +25% H_2 +50%Ar)	4	2	01/19	2P0119
							02/18	2P0218
							05/15	2P0515
						8	Continuous	2C
							02/18	8P0218
							Continuous	8C

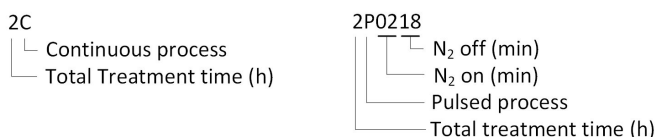


Figure 1. Example of specimen codification.

The layer thickness measurement and the chemical analysis by means of energy-dispersive X-ray spectroscopy (EDS) were made in with the aid of a Zeiss EVO-MA15 scanning electron microscope (SEM). The equipment belongs to the Multi-user Center for Materials Characterization (CMCM) of Federal University of Technology - Paraná, Curitiba Campus.

Before SEM analyses, specimens were transversely cut, wrapped in copper tapes and then mounted in high hardness resin (Bakelite). After mounting, specimens were ground with emery paper, polished and ultrasonic cleaned. They were then chemically etched with Marble reagent (4 g $\text{CuSO}_4 + 20 \text{ ml HCl} + 20 \text{ ml H}_2\text{O}$) in order reveal both nitrided layer and core microstructure.

The nitrogen concentration within the nitrided layer was determined by the method proposed by Öztürk and Williamson²³. According to this method, the amount of nitrogen is based on the lattice expansion, which can be determined by the shift of peaks corresponding to the austenite phase ($\gamma \rightarrow \gamma_N$, where γ is the unexpanded austenite phase, and γ_N is the expanded austenite phase). Equations 1 and 2 should be used in order to calculate the nitrogen concentration:

$$a_{\gamma_N} = a_{\gamma} + \alpha C_N \quad (1)$$

$$d_{hkl} = \frac{a}{\sqrt{h^2 + k^2 + l^2}} \quad (2)$$

where:

a_{γ} = lattice parameter of austenite [Å];

C_N = nitrogen concentration [at. %].

α = Vegard constant (considered value: 0.0078 [Å / at. %N]);

$a_{\bar{a}_N}$ = lattice parameter of expanded austenite [Å];

d_{hkl} = interplanar spacing.

3. Results and Discussion

3.1 Layer thickness measurements

The nitrided layers micrographs obtained by SEM are shown in Figure 2. It is possible to observe that, for all conditions, a double layer is present, where the outer layer is nitrogen-rich (γ_N) and the inner one is carbon-rich (γ_C)^{5,16,21}.

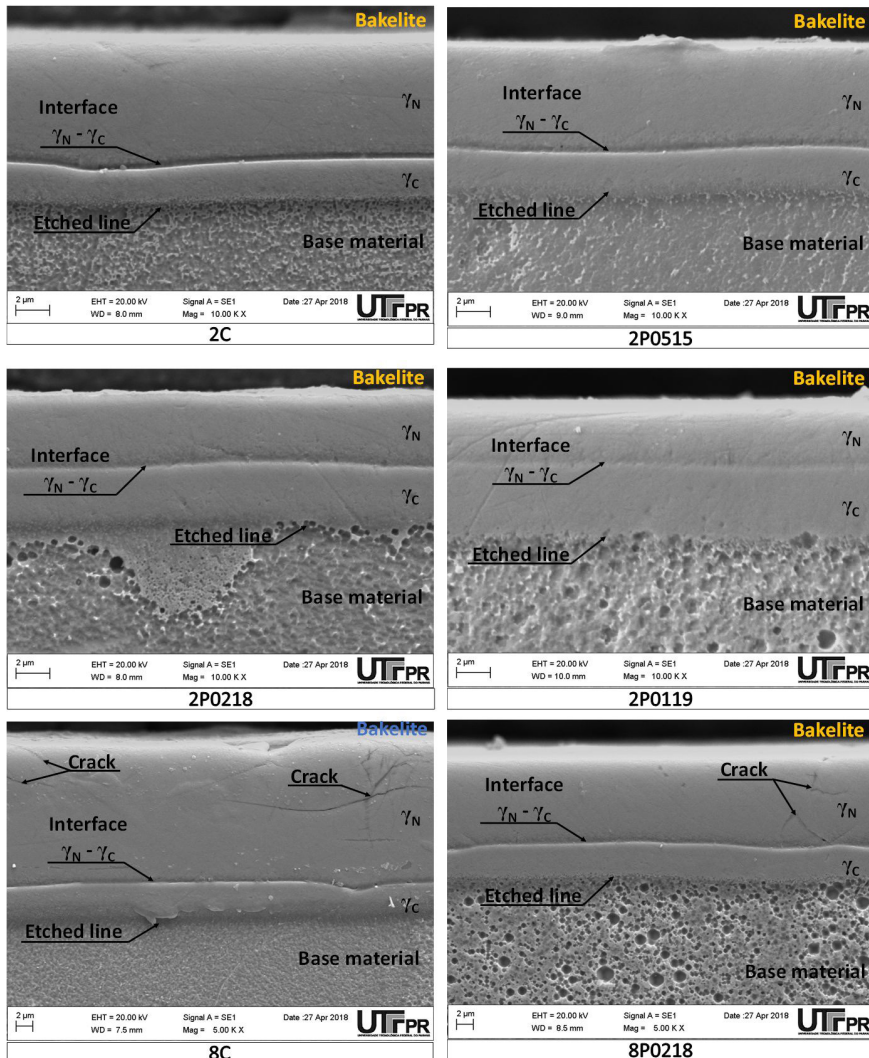


Figure 2. Micrographs of the nitrided layer taken in the SEM. Etching reagent: Marble.

Similar results were obtained in previous work, where the nitriding process were carried out at 450°C²². Nitrogen and carbon concentration profiles measured by GDOES by Sphair et al.²¹ showed that there is a high concentration of nitrogen close to the material surface, and a significant decrease at distances around 7 to 10 μm from the surface. Regarding carbon concentration, there is a maximum at about 7 to 11 μm from the surface. Even though this concentration is low, according to Sphair²¹ it can be about 8 times higher than the carbon concentration of the base material. Such higher carbon concentration is due to the introduction of nitrogen at the material surface, which forces the carbon to diffuse to the inner layer^{16,23}.

The thicknesses of outer, inner, and total layers were measured, and the results are shown in Table 3. It can be observed that the thickness of γ_N increases with increasing treatment times^{8,13,24}, and decreases when intermittent nitrogen flow is used²². When comparing the thicknesses values with those obtained by Sphair²¹, who reported layer thicknesses of 6.4 μm for the condition 2C and 5.0 μm for the condition 2P0218, both obtained at 400°C, it observed that the increase in temperature to 425°C resulted in a significant increase of the nitrided layer thickness.

The increase in temperature also increases the diffusion coefficient, favoring the growth of the nitrided layer. It must be considered that the plasma reactor used in this work do not have an auxiliary heating system, so the power of the high tension source must be raised in order to increase nitriding temperature. Because of this power increase, the concentration of nitriding species onto the material surface is higher, favoring even more the growth of the nitrided layer. Besides that, the formation of the expanded austenite layer, which is metastable, is a very complex phenomenon. Mändl et al.²⁵ reported that the diffusion coefficient of nitrogen in expanded austenite varies even with the nitrogen concentration.

According to Table 3, the total layer thickness for the condition 2C in this work is 11.0 μm, however, Reis et al.² obtained a value of 14.0 μm; such difference is due to the difference in process temperatures, which were 425°C and 450°C, respectively. Regarding the reduction in thickness of the γ_N layer with the use of pulsed nitrogen flow, both works obtained similar results. When it comes to the total layer thickness, it can be observed that, for specimens nitrided under continuous nitrogen flow, the thickness is higher when the total treatment time is considered. Since this a diffusion

dependent process, thicker layers are obtained for longer treatment times, for both continuous or intermittent nitrogen flow. For the specimens treated during 2h under intermittent nitrogen flow, it was verified that specimens 01/19 and 02/18 are very similar, but there is a clear trend regarding increase in layer thickness considering specimen 05/15.

The times of nitrogen flow on are 0.5 minutes (P0119), 1.5 minutes (P0218), and 4.5 minutes (P0515). The nitrided layer thickness should increase accordingly. When the flow is turned off, the chemical potential of the nitriding species drops to zero. As a consequence, the nitrogen close to the material surface is lost to the atmosphere²⁶, while remaining nitrogen diffuses inwards. Hence, the nitrogen concentration in the layer decreases. As shown by Mandl et al.²⁵, the diffusion coefficient varies with the concentration. When the growth of γ_N and γ_C layers are analyzed individually, is observed that the γ_N layer grows with increasing nitrogen flow times for all conditions, while the thickness of the γ_C layer tends to decrease as the nitrogen flow time increases. As a result, the total layer thickness ($\gamma_N + \gamma_C$) is the same for conditions 2P0119 e 2P0218. This fact must be related to the cleaning of the plasma reactor, since the carbon comes from the reactor walls, as pointed out by Czerviec et al.¹⁶. As the nitrogen flow time decreases, the carbon concentration at the material surface increases, favoring its diffusion, mainly at the beginning of the process, when the carbon concentration at the reactor walls is higher.

According to Czerviec¹⁶, the γ_C is formed because of carbon that is released from the reactor walls because of the in situ cleaning process, which is carried out with argon plasma before the nitriding process. In the present work, the γ_C layer was thicker for the intermittent nitrogen flow cycles. This indicates that the γ_C layer grows even during the nitriding process, probably when the nitrogen flow remains turned off. When the nitrogen flow is turned off, the argon present in the nitriding atmosphere releases carbon from the reactor walls, which eventually reaches the specimen surface and diffuses into the inner layer. When the nitrogen flow is turned on, some of the carbon released from the reactor walls reacts with nitrogen, forming CN, which, in its turn, is eliminated from the atmosphere by the vacuum system. This behavior is similar to those reported by Reis et al.²² and Sphair²¹.

Figure 3 shows cross-sections micrographs of specimens 8C and 8P0218. Cracks and layer detachment are observed in both conditions; however, the micrographs show that there

Table 3. Layer thickness for all treatment conditions.

Sample	Inner layer - γ_C (μm) Sphair (400°C)	Inner layer - γ_C (μm) (425°C)	Inner layer - γ_C (μm) Reis (450°C)	Outer layer - γ_N (μm) Sphair (400°C)	Outer layer - γ_N (μm) (425°C)	Outer layer - γ_N (μm) Reis (450°C)	Total thickness - $\gamma_N + \gamma_C$ (μm) Sphair (400°C)	Total thickness - $\gamma_N + \gamma_C$ (μm) (425°C)	Total thickness - $\gamma_N + \gamma_C$ (μm) Reis (450°C)
2P0119	-	4.6±0.4	-	-	3.4±0.5	-	-	8.0±0.1	-
2P0218	2.1±0.1	3.6±0.3	-	2.9±0.1	4.2±0.4	-	5.0±0.03	7.8±0.2	-
2P0515	-	3.0±0.3	-	-	5.6±0.4	-	-	8.6±0.1	-
2C	1.7±0.2	2.4±0.2	2.2 ± 0.3	4.7±0.3	8.6±0.3	11.8 ± 0.3	6.4±0.3	11.0±0.2	14.0 ± 0.4
8P0218	-	4.7±0.2	-	-	10.5±0.8	-	-	15.2±0.6	-
8C	-	4.2±0.2	-	-	18.6±1.0	-	-	22.8±0.8	-

are less defects in the nitrided layer formed with the use of pulsed nitrogen flow (8P0218). This could be explained by the smaller expansion of the austenite, which, in its turn, leads to less residual stresses within the layer^{5,8,10,12,14,18}. This assumption is in agreement with the results obtained by XRD and layer hardness, which are shown in the following topics.

3.2 X-ray Diffraction (XRD)

Results from X-ray diffraction are shown in Figure 4. From these results, it is possible to observe that the austenite (γ) peaks have shifted to the left when compared to the as-received (solubilized) specimen, indicating the formation of expanded austenite (γ_N)^{1,4,5,7,8,11-13,17,18,24}. The peaks corresponding to expanded austenite are broader than those of non-expanded austenite from the starting material. This broadening is caused by crystal defects, nitrogen concentration gradients, and the presence of residual stresses in the layer^{6,11,24}. Prior

to nitriding, the material (ISO 5832-1 steel) was solubilized at 1180°C for 2 hours. Thus, the results regarding nitrogen concentration, which are given by the lattice expansion as proposed by Öztürk and Williamson²³, were not affected by residual stresses in the material before nitriding. This method considers that the lattice expansion, and consequent generation of residual stresses, is due to the nitrogen introduction during the nitriding process.

When comparing specimens treated under continuous nitrogen flow for different times, 2C and 8C, there was no difference regarding austenite expansion. This indicates that the solubility limit was reached, and above this point the nitrogen tends to precipitate in the form of nitrides. The concentration of nitrogen into the expanded austenite layer is higher when continuous flow is used (Figure 5). The higher the nitrogen concentration, the higher the tendency of formation of nitrides. As shown by Mändl et al⁵, the diffusion coefficient

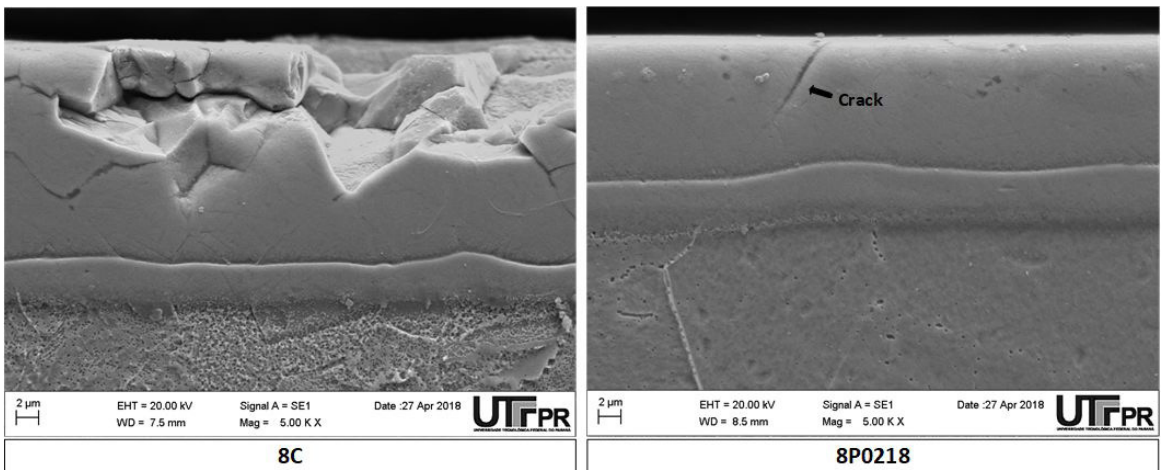


Figure 3. Comparison of treated surfaces in continuous (8C) and pulsed (b) process.

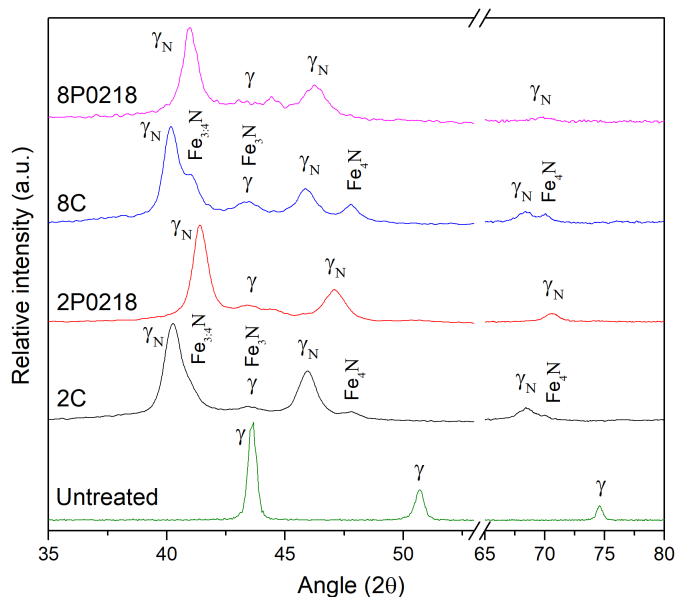


Figure 4. Diffraction patterns of untreated and nitrided samples.

decreases when the lattice is saturated with nitrogen. Since the expanded austenite is a metastable phase, and when it is saturated, regions of high energy, such as grain boundaries, favor the phase transformation and consequent precipitation of nitrides. When the nitrogen flow is pulsed, the nitrogen concentration decreases (Figure 5) because of diffusion, reducing the tendency of precipitation of nitrides. Thus, similar amounts of nitrogen in solid solution are observed for both conditions²⁷, with higher precipitation of nitrides for specimen 8C compared to specimen 2C. It is observed that the intensity of the peaks related to those phases is

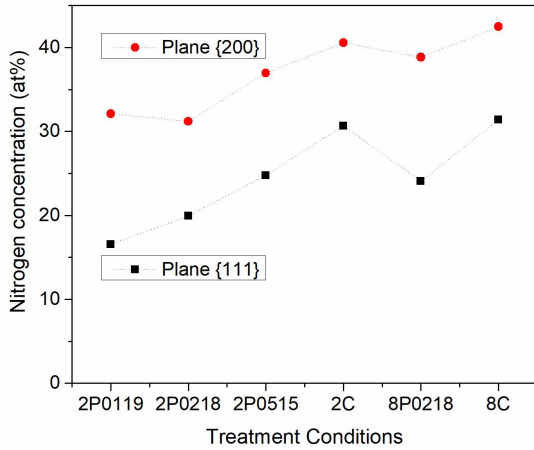


Figure 5. Nitrogen concentration in atomic percentage calculated by means of equations 1 and 2.

higher for the condition 8C. For the pulsed flow of nitrogen, there is a lower tendency of formation of precipitates, since when the gas flow is turned off, the nitrogen diffuses and its concentration within the layer is decreased. Hence, the tendency of nitrides precipitation is lower. In such conditions, no peaks related to those nitrides were observed; however, it is not possible to state that there was no formation of precipitates, since the size and amount of both chromium and iron precipitates may lie below the detection limits of the DRX technique²⁸.

When comparing the austenite expansion that occurred for condition 2C with the work of Reis et al.²², in which nitriding was carried out at 450°C, the results obtained in this work are very similar, indicating that the hypothesis that the solubility limit was reached is valid. It is also possible to see that the degree of precipitation is lower in the present work when compared to the work of Reis et al.²². As previously proposed, for treatments made with intermittent flow of nitrogen, the concentration of nitrogen within the layer is lower; hence, it was possible to increase treatment times up to nitrogen saturation, as opposed to what happened in the treatments with continuous nitrogen flow.

3.3 Energy Dispersive X-Ray Spectroscopy (EDS)

Figure 6 shows where EDS measurements were taken, and values of Cr, Ni, and Mo concentrations are shown in Table 4. From EDS results, it can be seen that the amount of chromium and molybdenum are higher, while the amount of nickel is lower at measurement point 1 when compared to measurement point 2 (reference point) for

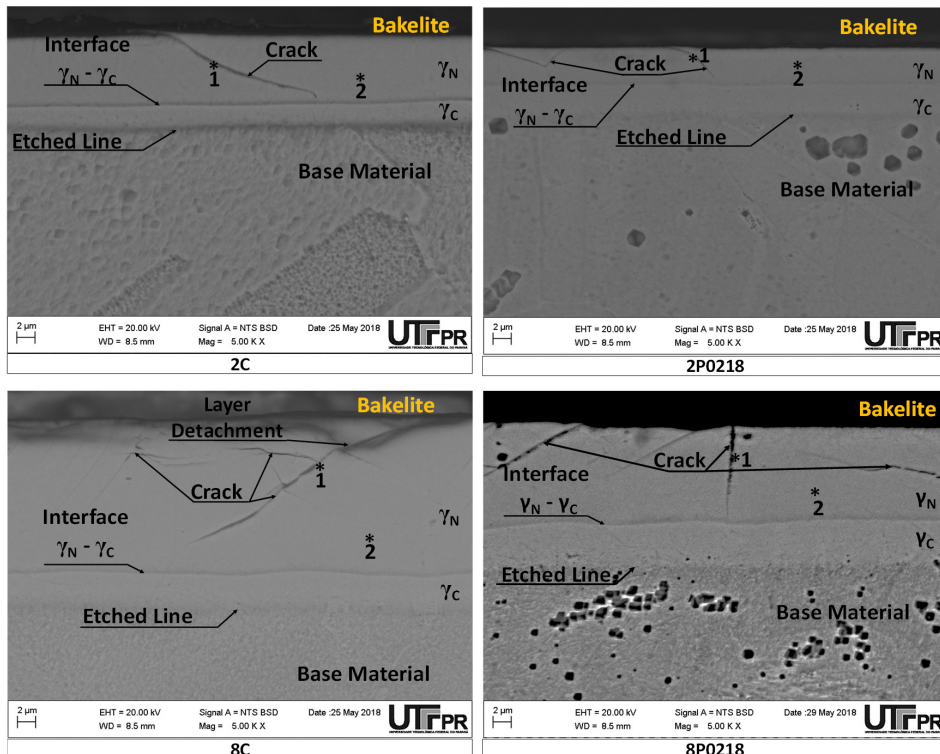


Figure 6. Images of energy dispersion spectroscopy analysis for all treatment conditions.

Table 4. Weight relative percentage of chromium, molybdenum and nickel in the nitrided layer.

Sample	Measurement point	%Cr	%Mo	%Ni
2C	1	20.7	3.2	13.7
	2	15.5	2.2	17.4
2P0218	1	17.9	2.4	17.4
	2	16.5	2.5	17.3
8C	1	23.0	5.1	9.6
	2	16.5	2.5	17.4
8P0218	1	17.7	2.9	15.0
	2	15.0	2.3	16.2

specimens 2C and 8C. Since chromium and molybdenum have chemical affinity with nitrogen^{2,3}, unlike nickel, these results indicate the formation of nitrides in regions close to the grain boundaries. The differences in measurements taken at point 1 and point 2 are higher for specimen 8C, indicating that the precipitation of nitrides was more intense for this specimen than for 2C. Regarding specimens 2P0218 and 8P0218, no changes in chromium, molybdenum and nickel amounts were observed, which may indicate that the size of the precipitates is too small and below detection limits of the EDS technique. In previous work²², with a process temperature of 450°C, chromium precipitates were detected for all process conditions. These results are in agreement with the literature^{6,9,11,17}, indicating that the formation of chromium-based nitrides is influenced not only by the nitrogen concentration, but also by the process temperature.

3.4 Nanohardness

Hardness measurements were made with the nanoindentation technique, and obtained results are shown in Table 5. It is observed that the hardness of specimens treated with intermittent nitrogen flow is slightly lower than those of the specimens treated with continuous nitrogen flow for the same total treatment time. Shorter time treatments (both intermittent or continuous nitrogen flow) led to lower hardness values when compared to longer time treatments. Such results are related to the smaller lattice expansion, as confirmed by the XRD analyses, which resulted in less residual stresses within the layer. This behavior is similar to that reported by Reis et al.²

The microhardness of the layer treated according cycle 2C at 450°C measured by Reis et al.²² was similar to that obtained in the present work, which are 12.86 GPa and 13.35 GPa, respectively. Considering the intermittent nitrogen flow conditions, a great difference in hardness values is observed. Hardness values of specimens treated at 450°C are smaller than for specimens treated at 425°C. This apparent incoherence may be explained by the influence of the layer thickness in the hardness measurement as well as the technique that was used in both works. Reis et al.²² measured layer thickness using microhardness techniques, while in the present work the nanoindentation technique was used. Since the hardness value is a result of the interaction between the hardness of the layer and the material substrate, higher values are measured when the influence of the substrate hardness is diminished. When the nanoindentation technique is used, the influence of the

Table 5. Surface nanohardness of the pulsed and continuous process for 2C, 2P0218, 8C, and 8P0218 samples.

Sample	Hardness (GPa)
2C	13.35 ±1.68
2P0218	12.03 ±0.48
8C	13.54 ±2.31
8P0218	12.79 ±0.25

substrate is significantly lower, because of the magnitude of the loads used in the measurement process. Considering treatments made with intermittent nitrogen flow where thinner layers are produced, the substrate influence in the hardness values increase, which justifies the differences observed between these two works.

Even though the effective time of nitrogen flow is much shorter for the intermittent flow treatments, specimens 2P0218 and 8P0218 treated in those conditions had a hardness that is only slightly lower than those treated with continuous nitrogen flow. On the other hand, it is possible to infer that the residual stresses level in the nitrided layers obtained by continuous nitrogen flow is significantly higher, mainly because of the cracks and surface damage shown previously in SEM micrographs.

4. Conclusions

From the results obtained in this work, it is possible to conclude that the expanded austenite (γ_N) phase was formed for all treatment conditions, and that its thickness increase with treatment time and decreases when intermittent nitrogen flow is used during nitriding. The precipitation of chromium nitrides is higher for specimens treated with continuous nitrogen flow. Hardness measurements showed that the layer formed with intermittent nitrogen flow is slightly lower because of smaller expansion of the austenite as a result of the lower nitrogen concentration in that phase. Overall, it is possible to conclude that the use of pulsed nitrogen flow allowed to control the nitrogen concentration in the expanded austenite phase, with lower residual stresses within the nitrided layer, less residual stresses and lower amount of precipitates that might compromise the corrosion resistance of the material. When compared to the work of Reis et al.²², results indicate that the reduction in process temperature from 450°C to 425°C led to different degrees of chromium-based precipitation within the nitrided layer.

5. Acknowledgements

The authors would like to thank Villares Metals for the donation of the material employed in the research, Araucaria Foundation for scientific initiation scholarship, and CNPq for financial support (CNPq Project 430088/2016-7), and Multi-User Center for Materials Characterization - CCMC of UTFPR-CT.

6. References

1. Asgari M, Barnoush A, Johnsen R, Hoel R. Microstructural characterization of pulsed plasma nitrided 316L stainless steel. *Mater Sci Eng A*. 2011;529:425-34. <http://dx.doi.org/10.1016/j.msea.2011.09.055>.
2. Borgioli F, Fossati A, Galvanetto E, Bacci T. Glow-discharge nitriding of AISI 316L austenitic stainless steel: influence of treatment temperature. *Surf Coat Tech*. 2005;200(7):2474-80. <http://dx.doi.org/10.1016/j.surfcoat.2004.07.110>.
3. Borgioli F, Galvanetto E, Bacci T. Low temperature nitriding of AISI 300 and 200 series austenitic stainless steels. *Vacuum*. 2016;127:51-60. <http://dx.doi.org/10.1016/j.vacuum.2016.02.009>.
4. Buhagiar J, Dong H, Bell T. Low temperature plasma surface alloying of medical grade austenitic stainless steel with carbon and nitrogen. *Surf Eng*. 2006;151:446. <http://dx.doi.org/10.1007/BF03165205>.
5. Gontijo LC, Machado R, Casteletti LC, Kuri SE, Nascente PAP. Comparação entre os comportamentos dos aços inoxidáveis AISI 304L e AISI 316L nitretados a plasma. *Rev Bras Apl Vácuo*. 2007 [cited 2020 Sept 06];26(3):145-50. Available from: www.sbvacu.org.br/rbav/index.php/rbav/article/download/37/35
6. Larisch B, Brusky U, Spies HJ. Plasma nitriding of stainless steels at low temperatures. *Surf Coat Tech*. 1999;116-119:205-11. [http://dx.doi.org/10.1016/S0257-8972\(99\)00084-5](http://dx.doi.org/10.1016/S0257-8972(99)00084-5).
7. Dos Reis RF, Maliska AM, Borges PC. Nitretação à plasma do aço inoxidável austenítico ISO 5832-1: influência do tempo de tratamento. *Materia (Rio J)*. 2008;13(2):304-15. <http://dx.doi.org/10.1590/S1517-70762008000200008>.
8. Stinville JC, Villechaise P, Templier C, Riviere JP, Drouet M. Plasma nitriding of 316L austenitic stainless steel: experimental investigation of fatigue life and surface evolution. *Surf Coat Tech*. 2010;204(12-13):1947-51. <http://dx.doi.org/10.1016/j.surfcoat.2009.09.052>.
9. Yazıcı M, Çomaklı O, Yetim T, Yetim AF, Çelik A. The effect of plasma nitriding temperature on the electrochemical and semiconducting properties of thin passive films formed on 316L stainless steel implant material in SBF solution. *Surf Coat Tech*. 2015;261:181-8. <http://dx.doi.org/10.1016/j.surfcoat.2014.11.037>.
10. Yetim EF, Yildiz F, Alsarhan A, Çelik A. Surface modification of 316L stainless steel with plasma nitriding. *Kovove Mater*. 2008 [cited 2020 Sept 06];46(2):105-15. Available from: <https://www.researchgate.net/publication/273452215>
11. Liang W. Surface modification of AISI 304 austenitic stainless steel by plasma nitriding. *Appl Surf Sci*. 2003;211:308-14. [http://dx.doi.org/10.1016/S0169-4332\(03\)00260-5](http://dx.doi.org/10.1016/S0169-4332(03)00260-5).
12. Mendes AF, Scheuer CJ, Joanidis IL, Cardoso RP, Mafra M, Klein NA, et al. Low-temperature plasma nitriding of sintered PIM 316L austenitic stainless steel. *Mater Res*. 2014;17(1):100-9. <http://dx.doi.org/10.1590/S1516-14392014005000064>.
13. Templier C, Stinville JC, Villechaise P, Renault PO, Abroniss G, Rivière JP, et al. On lattice plane rotation and crystallographic structure of the expanded austenite in plasma nitrided AISI 316L steel. *Surf Coat Tech*. 2010;204(16-17):2551-8. <http://dx.doi.org/10.1016/j.surfcoat.2010.01.041>.
14. Baranowska J, Arnold B. Corrosion resistance of nitrided layers on austenitic steel. *Surf Coat Tech*. 2006;200(22-23):6623-8. <http://dx.doi.org/10.1016/j.surfcoat.2005.11.099>.
15. Tschiptschin AP, Pinedo CE. Estrutura e propriedades do aço inoxidável austenítico AISI 316L grau ASTM F138 nitretado sob plasma à baixa temperatura. *Revista Escola de Minas*. 2010;63(1):137-41. <http://dx.doi.org/10.1590/S0370-44672010000100023>.
16. Czerwicz T, He H, Weber S, Dong C, Michel H. On the occurrence of dual diffusion layer during plasma-assisted nitriding of austenitic stainless steel. *Surf Coat Tech*. 2006;200:5289-95. <http://dx.doi.org/10.1016/j.surfcoat.2005.06.014>.
17. Mingolo N, Tschiptschin AP, Pinedo CE. On the formation of expanded austenite during plasma nitriding of an AISI 316L austenitic stainless steel. *Surf Coat Tech*. 2006;201(7):4215-8. <http://dx.doi.org/10.1016/j.surfcoat.2006.08.060>.
18. Mändl S, Rauschenbach B. Nitrogen Diffusion in Austenitic Stainless Steel and the Formation of Expanded Austenite. *Defect and Diffusion Forum*. 2001 [cited 2020 Sept 06];188:125-36. Available from: www.scientific.net/DDF.188-190.125
19. Menthe E, Bulak A, Olfé J, Zimmermann A, Rie KT. Improvement of the mechanical properties of austenitic stainless steel after plasma nitriding. *Surf Coat Tech*. 2000;133-134:259-63. [http://dx.doi.org/10.1016/S0257-8972\(00\)00930-0](http://dx.doi.org/10.1016/S0257-8972(00)00930-0).
20. Bernardelli EA, Borges PC, Fontana LC, Floriano JB. Role of plasma nitriding temperature and time in the corrosion behaviour and microstructure evolution of 15-5 PH stainless steel. *Kovové Materiály*. 2010;48:105-16. http://dx.doi.org/10.4149/km_2010_2_105.
21. Sphair AC. Nitretação por plasma de aço inoxidável austenítico com fluxo pulsado de nitrogênio [dissertação]. Curitiba: Universidade Tecnológica Federal do Paraná; 2017. [cited 2020 Sept 06]. Available from: <http://repositorio.utfpr.edu.br/jspui/handle/1/2970>
22. Dos Reis RF, Da Silva PGHM, Villanova RL, Vianna AM, Bernardelli EA. Plasma nitriding of ISO 5832-1 stainless steel with intermittent nitrogen flow at 450 °C. *Mater Res*. 2020;23(1). <http://dx.doi.org/10.1590/1980-5373-mr-2019-0501>.
23. Öztürk O, Williamson DL. Phase and composition depth distribution analyses of low energy, high flux N implanted stainless steel. *J Appl Phys*. 1995;77:3839. <http://dx.doi.org/10.1063/1.358561>.
24. Wang L, Ji S, Sun J. Effect of nitriding time on the nitrided layer of AISI 304 austenitic stainless steel. *Surf Coat Tech*. 2006;200(16-17):5067-70. <http://dx.doi.org/10.1016/j.surfcoat.2005.05.036>.
25. Mandl S, Scholze F, Neumann H, Rauschenbach B. Nitrogen diffusivity in expanded austenite. *Surf Coat Tech*. 2003;174-175:1191-5. [http://dx.doi.org/10.1016/S0257-8972\(03\)00454-7](http://dx.doi.org/10.1016/S0257-8972(03)00454-7).
26. Steiner T, Meka SR, Göhring H, Mittemeijer EJ. Alloying element nitride stability in iron-based alloys; denitriding of nitrided Fe-V alloys. *Mater Sci Technol*. 2017;33(1):23-32. <http://dx.doi.org/10.1080/02670836.2016.1155254>.
27. Heras EDL, Ybarra G, Lamas D, Cabo A, Dalibon EL, Bruhl SP. Plasma nitriding of 316L stainless steel in two different N₂-H₂ atmospheres - Influence on microstructure and corrosion resistance. *Surf Coat Tech*. 2017;313:47-54. <http://dx.doi.org/10.1016/j.surfcoat.2017.01.037>.
28. Zagonel LF, Bettini J, Basso RLO, Paredes P, Pinto H, Lepienski CM, et al. Nanosized precipitates in H13 tool steel low temperature plasma nitriding. *Surf Coat Tech*. 2012;207:72-8. <http://dx.doi.org/10.1016/j.surfcoat.2012.05.081>.